

# **SIMULATION OF HYDROGEN DISPERSION UNDER CRYOGENIC RELEASE CONDITIONS**

**Giannissi, S.G.<sup>1,2</sup>, Venetsanos, A.G.<sup>1</sup>, Markatos, N.<sup>2</sup> and Willoughby, D.B.<sup>3</sup>, Royle, M.<sup>4</sup>**

**<sup>1</sup> Environmental Research Laboratory, National Center for Scientific research Demokritos, Aghia Paraskevi, Athens, 15310, Greece, [sgiannissi@ipta.demokritos.gr](mailto:sgiannissi@ipta.demokritos.gr),**

**[venets@ipta.demokritos.gr](mailto:venets@ipta.demokritos.gr)**

**<sup>2</sup> National Technical University of Athens, Scholl of Chemical Engineering, Department of Process Analysis and Plant Design, Heron Polytechniou 9, 15780, Athens, Greece, [n.markatos@ntua.gr](mailto:n.markatos@ntua.gr)**

**<sup>3</sup> Health and Safety Laboratory, Buxton, Derbyshire, SK17 9JN, United Kingdom, [deborah.willoughby@hsl.gsi.gov.uk](mailto:deborah.willoughby@hsl.gsi.gov.uk)**

**<sup>4</sup>Health and Safety Executive, Bootle Merseyside L20 7HS, United Kingdom, [mark.royle@hse.gsi.gov.uk](mailto:mark.royle@hse.gsi.gov.uk)**

## **ABSTRACT**

The use of hydrogen as fuel should always be accompanied by a safety assessment, in case of an accidental release. To evaluate the potential hazards in a spill accident both experiments and simulations are performed. In the present work, the CFD code, ADREA-HF, is used to simulate the liquefied hydrogen (LH2) spill experiments (test 5, 6, 7) conducted by the Health and Safety Laboratory (HSL). In these tests, LH2 was spilled at a fixed rate of 60lt/min in several directions and for several durations. The factors that influence the vapor dispersion under cryogenic release conditions that were examined in this study are: the air humidity, the wind direction, and the slip effect of droplets formed by both the cryogenic liquid and the condensation of air humidity. The numerical results were compared with the experimental measurements, and the effect of each abovementioned factors in the vapor dispersion is being discussed.

## **1.0 INTRODUCTION**

Hydrogen is a competitive fuel in the energy market due to its high energy carrier and low emissions. However, its wide flammability range brings up safety issues. Hydrogen storage and handling demands its liquefaction under pressure and low temperature. In case of a fracture in the cryogenic tank, LH2 is spilled forming a cryogenic pool and a dense gas cloud. The jet release is two phase and prediction of both vapour dispersion and liquid pool evaporation and spreading is required. Computational Fluid Dynamics (CFD) codes are usually used to simulate such complicated cases.

In the present work, ADREA-HF is used to simulate the HSL experiments [1] related to hydrogen dispersion under cryogenic release conditions. ADREA-HF is a CFD code that has been validated against hydrogen dispersion and other liquefied fuels such as natural gas, or denser than air gases [2-12], and it is considered to be a useful tool for such applications.

During HSL experiments LH2 was released above a concrete pad at a fixed rate of 60lt/min. Four tests were performed with different release directions and duration. Wind speed and direction were measured at the edge of the pad 2.5 m from the ground. Sensors that measured the temperature were deployed in line with the release at several distances and heights. The hydrogen concentration was derived by the temperature data assuming adiabatic mixing. Thermocouples inside the ground measured also the underground temperature.

The parameters that influence the hydrogen dispersion are various, especially when the release takes place in an open environment. Apart from the release conditions significant role play the wind speed and direction, the atmospheric conditions, the air moisture, the ground terrain, etc. The present work focuses on the effect of air moisture and wind direction on vapor dispersion. The computational results are compared with the measurements for test 5, 6, and 7 that are chosen to be simulated.

Another factor that should be examined is the effect of the liquid phase of both hydrogen and condensed humidity, and of the solid phase of ice crystals produced by the solidification of atmospheric humidity on the flow. The liquid and solid phases develop a different velocity from the vapour phase due to the density difference. The difference between the phases' velocity is called slip velocity. In the present study the slip effect is examined for test 5 and 6.

## 2.0 DESCRIPTION OF THE EXPERIMENTS

The HSL experiments were conducted by the Health and Safety Laboratory in 2010. During these experiments LH2 was spilled above a concrete pad in open environment. A number of tests were performed in which LH2 was released either horizontally along the ground, or, vertically downwards 100mm above ground, or horizontally 860 mm above the ground. The absolute storage pressure in the tank was 2 bars and the absolute release pressure was 1.2 bars for all test cases.

The release rate was 60lt/min in each test and the release duration was ranged from 265 to 561 sec. The wind speed varied between 1.4 and 3.35 m/s at 2.5 m height. The wind direction fluctuated around the average wind direction, which was approximately in line with the release for each test. The relative atmospheric humidity varied from 65 to 87%.

For test 5, 6, and 7 sensors were placed in line with the release at 1.5, 3, 4.5, 6, 7.5 m downwind the spill point, and 0.25, 0.75, 1.25, 1.75, 2.25, and 2.7 m above the ground. For test 10, thirty sensors were positioned at a range of heights and distances around the spill point.

Table 1 presents the release and weather conditions for tests 5, 6, and 7 which are simulated in the present work.

Table 1. Release and Weather Conditions for test 5, 6, 7.

	TEST 5	TEST 6	TEST 7
spill diameter (mm)	26.6	26.6	26.6
source height (mm)	3.36	100	860
source direction	Horizontal (x-direction)	Vertical (w-direction)	Horizontal (x-direction)
release rate (kg/sec)	0.07	0.07	0.07
release duration (sec)	248	556	305
average wind speed (@ 2.5 m ) (± standard deviation)	2.675 ± 0.09	3.36 ± 0.95	3.07 ± 0.82
average wind direction (@ 2.5m) (± standard deviation)	291 ± 15.5	295 ± 13.4	294.5 ± 14
average ambient temperature (@2.5m)	283	283	283
ambient relative humidity (%)	68	68	64

## 3.0 SIMULATION PROCESS

### 3.1 ADREA-HF code

ADREA-HF code is a three dimensional time dependent finite volume CFD code that has been successfully used for prediction of pollutants and hazardous gases dispersion in open and closed environments. The main focus has been given to prediction of hydrogen dispersion for both cryogenic and compressed releases [5]-[8]. In general, ADREA-HF is considered to be an appropriate and useful tool for risk assessment of hydrogen and other gases applications.

ADREA-HF software solves the Navier-Stokes equations for the mixture, either using homogeneous equilibrium model, or permitting the liquid and gas phase to have different velocities by using extra slip terms in the conservation equations. Coupled with the Navier-Stokes equations the mass and energy conservation equations are solved.

In ADREA-HF code a variety of turbulence models is available. There are RANS turbulence models of zero equation (e.g. mixing length), one equation and two equations (e.g. standard k- $\epsilon$ , RNG k- $\epsilon$ ), and LES models. In the present work, k- $\epsilon$  model is used with extra source terms for buoyancy [13-14].

### 3.2 Modeling approach

Test 5, 6, and 7 of the HSL experiments are simulated. In all tests the source is modeled as a two phase jet. The percentage of vapor phase is calculated assuming isenthalpic expansion from the storage pressure to the release pressure. The spill velocity is calculated using the source area and the mixture density of the two phase jet, and it is approximately 6m/s for each test.

Both vapor and liquid hydrogen coexist in the domain, until all the liquid hydrogen has been evaporated by absorbing heat. The heat source is the ambient air and the ground. No solar radiation is taken into account. The computational code, as mentioned above, solves for the mixture, and not for each phase separately. For the phase distribution in the mixture is assumed that the liquid phase appears, when the mixture temperature is equal or lower than the dew temperature of the mixture [15]. In case that the mixture temperature drops below the freezing point of a component, then the solid phase of that component appears.

The liquid and solid phases are dispersed with the vapor phase in each cell. If liquid hydrogen is predicted in a boundary cell (cell on the ground) during the simulation, it is assumed that the area of that cell projected to the ground is the area of the liquid pool. In this way the pool formation and spreading is computed.

The presence of atmospheric humidity makes the cloud more buoyant due to the heat liberation by the water's condensation and solidification. The effect of the air humidity on the gas dispersion is examined in the present study. The air humidity is taken into account by solving an additional mass fraction conservation equation for the water. The water mass fraction of the air is calculated from the measured relative humidity, and it is 0.00529 for test 5, 6 and 0.00532 for test 7.

When spill takes place in open environment, the wind has major effect on the gas dispersion. The air entrainment in the cloud spreads it downwind towards the wind direction. Although, the average wind direction in HSL experiments is in alignment with the release, many oscillations in the measured hydrogen concentration were observed. That fact led us to the conclusion that the effect of the instantaneous direction plays a larger role than is was initially expected.

Fig.1 shows the  $v$  component of wind velocity ( $y$ -direction) in conjunction with the hydrogen concentration at 1.5 m downwind the release and 0.25 m height for test 5. The measured  $v$ -component was computed by multiplying the wind speed magnitude by the sine of the angle of the wind direction in each time. As shown in the figure the  $v$ -velocity fluctuates constantly around the value of zero. At first, one can consider that taking an average value of the  $v$ -component equal to zero would be a good approximation. However, the oscillations of the measured hydrogen concentration objected to that simplification. The statement that wind direction affects the gas dispersion is supported by Figure 1, where it seems that when the  $v$ -component is positive the concentration reaches a peak and when it is negative the concentration falls down. That is happening because as wind changes direction the cloud is shifted to its direction. Similar behavior is observed also in test 6 and 7. Therefore, the effect of the wind direction on the prediction will be examined in the present study.

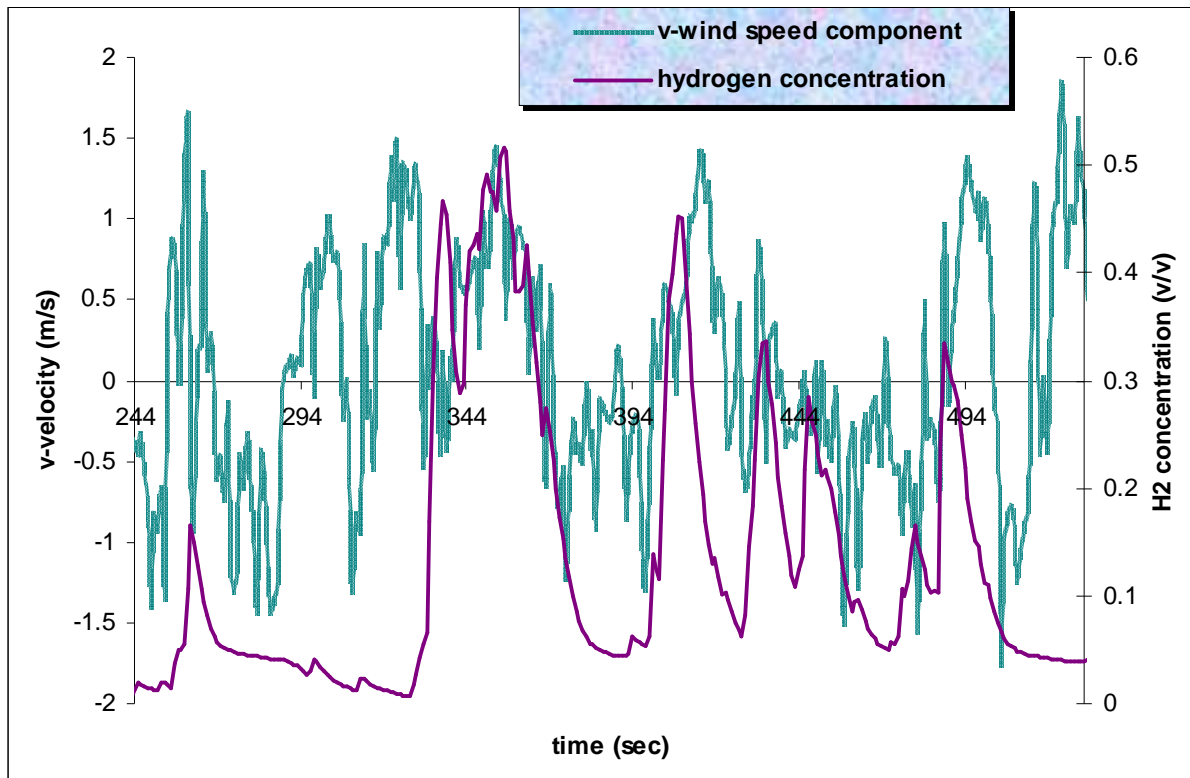


Figure 1. The measured v-component of the wind speed and the measured hydrogen concentration at sensor 10 ( $x=1.5\text{m}$ ,  $y=0\text{m}$ ,  $z=0.25\text{m}$ - in respect with the release point located at  $x=0$ , and  $y=0$ , and the ground level at  $z=0$ ) for test 5.

In the simulation process the wind field was calculated as following: One dimensional steady problem was solved, in order to obtain the wind profile based on the average wind speed and direction. The calculated profile was set as initial wind field for the whole domain and as inflow values for all variables. In the case where the instantaneous direction was taken into account, the v-component of wind velocity was transient and its values were set on boundaries based on the measured values.

### 3.3 Computational domain and grid

The computational domain extended 15m in the x-direction (from 5 m upwind to 10m downwind of the release point), 20m in the y-direction (crosswind) and 10m in the z-direction in all three tests. The grid is Cartesian and consists of 93 840 cells ( $40 \times 69 \times 34$ ), 119 952 cells ( $63 \times 68 \times 28$ ) and 142 830 cells ( $45 \times 69 \times 46$ ) in test 5, 6, and 7 respectively. Refinement points are near the release and on the ground with minimum cell size equal to the source diameter in the cell that encloses the source and refinement factor 1.12 in all tests.

### 3.4 Boundary conditions

The west domain (upwind the release) was the inlet boundary. At the inlet boundary inflow (Dirichlet) conditions were imposed with values provided by the 1D steady state problem for all variables. In the case with transient wind direction the value of the v-velocity component in the inflow boundary was a function of time according to the measurements. In particular, linear functions were taken between the most discrete extrema. The v- component was uniform in the vertical direction. All other variables had the values that the 1D steady state problem provided.

The east domain (downwind the release) was outlet boundary. The outlet boundaries were prescribed by applying zero gradient for all variables except components' mass fraction and temperature, for which either a zero gradient boundary condition was applied if outflow occurs or a given value boundary condition (equal to the initial value) if inflow occurs.

The top boundary is a free boundary and symmetry boundary condition was applied. Therefore, the normal component of velocity was set equal to zero and for all other variables zero gradient boundary condition was imposed, except components' mass fraction and temperature, which boundary conditions were the same as the outlet boundary.

In the side boundaries (north and south domain) symmetry boundary condition was applied, since the domain was extended enough. In the case with transient wind direction the side boundaries were either inflow or outflow boundaries depending on the wind direction, and the respective boundary conditions were imposed during the simulation process.

On the bottom domain (ground) a wall boundary condition was applied with roughness length 2.4mm. The temperature at the bottom boundary is calculated by solving a transient one dimensional temperature equation in the underground. The depth of the underground should be taken deep enough to be able to assume that the temperature in the bottom of the underground is constant in time equal to the initial temperature. The minimum depth which the above assumption is applicable is calculated by the following relationship:

$$\delta = 4\sqrt{\alpha t} , \quad (1)$$

$$\text{and } \alpha = \frac{\lambda}{\rho c_p} \quad (2)$$

where  $\delta$  - the depth, m;  $\alpha$  - thermal diffusivity,  $\text{m}^2/\text{s}$ ;  $t$  - time, s.;  $\rho$  - density,  $\text{kg}/\text{m}^3$ ;  $c_p$  - heat capacity,  $\text{J}/\text{kg} \cdot \text{K}$ ;  $\lambda$  - thermal conductivity,  $\text{W}/\text{m} \cdot \text{K}$ .

In this work, the underground consists of two layers. The bottom layer is sandy ground and the upper layer is concrete. No experimental data for the concrete properties were available. The properties of the concrete used in the simulation were  $\rho = 2371 \text{kg}/\text{m}^3$ ,  $c_p = 880 \text{J}/\text{kg} \cdot \text{K}$  and  $\lambda = 1.13 \text{W}/\text{m} \cdot \text{K}$ , consequently  $\alpha = 5.41582 \cdot 10^{-7} \text{m}^2/\text{s}$ . Using these properties the minimum depth required is ranged from 0.058m to 0.083m for the three tests. So, the assumption of an underground depth equal to 1.5m and a concrete pad of 80mm thickness lies within boundaries.

The grid size of the underground temperature equation was tested. So, an underground grid independency study was performed. The grid independency in the underground has never been studied in the past, assuming that its effect would be small in the overall prediction. However, the study reveals a significant effect of the size of the minimum underground boundary cell on heat transfer, and consequently on the predicted concentrations. The grids that were tested consist of 10, 20, 30, 60, 90, and 120 equidistant cells. The independent grid was the one with 90 cells. Another grid was tested consisted of 10 cells with refinement factor of 1.45 and refinement point the surface ( $z=0$ ). This grid has the same minimum cell size as the independent grid, and the numerical results show the same behavior as the independent grid. Therefore, the grid with 10 cells and refinement was used in all the predictions.

### 3.5 The slip model

As mentioned in previous section the ADREA-HF code can solve the conservation equations for the mixture, either using homogeneous equilibrium model, or adding slip terms in the equations. In the code a variety of algebraic slip models is available. These slip models calculate the w-slip velocity as

function of non vapor mass fraction. The  $u$  and  $v$  slip velocity components are not currently calculated and are assumed equal to zero. This simplification is accepted because the contribution of  $w$ -slip is bigger compared to the other components, due to gravity acceleration. In the present study the Ogura and Takahashi empirical relation for water [16] is used. This means that the model does not distinguish between the non vapor hydrogen and the non vapor water, and treats them the same. This is acceptable because the area occupied by the liquid hydrogen is very small compared to the area occupied by the liquid/solid water. However, a more rigorous slip model should be examined.

#### 4.0 RESULTS AND DISCUSSION

Three cases were modeled and compared to each other and to the measurements for each HSL test. For test 5 and 6 one additional case (case 4) was examined. Table 2 shows these cases.

Table 2. Modeled cases.

No Case	Description
1	Homogeneous model - No humidity - Wind direction in line with the release
2	Homogeneous model - Humidity - Wind direction in line with the release
3	Homogeneous model - Humidity - Transient wind direction
4	Non homogeneous model (slip effect) - Humidity – Transient wind direction

For the sake of brevity, from this point each case will be mentioned with its number, instead of using the whole expression.

#### 4.1 Test 5

Fig. 2 compares the measured and predicted peak hydrogen concentration at distances downwind the release for all four cases. The results are in very good agreement with the measurements for case 4, while for case 1, 2 and 3 the model overpredicts the gas concentration at the lower sensors and underpredicts it at the higher sensors.

The dense cloud of case 1 spreads more in the horizontal direction rather than the vertical, predicting higher concentration levels in the lower sensors. The results for case 2 are little improved compared to case 1. The condensation and solidification of air humidity liberates heat and makes the cloud more buoyant. Concentration in low sensors decreased, while concentration in higher sensors increased, and the numerical results are closer to the experimental ones. Similar behavior is observed for case 3 as far as the concentration levels are concerned.

At this point it is necessary to mention that the condensation and solidification of the air components ( $N_2$  and  $O_2$ ) is expected to have little effect on the buoyancy of the cloud, because the area of the domain where the mixture temperature is below their boiling and freezing points is restricted to a zone near the release point. This remark is already mentioned in [17] for test-7, while for test-6 a strong influence of the air condensation was noted. On the contrary, the area where humidity condensed and solidified is much more extended, and provides the main contribution to the cloud buoyancy. However, to have a complete perception and to jump into conclusions the air condensation/solidification should be examined for test-5 too.

In case 4, in addition to the heat transfer from humidity phase change the slip effect also contributes to the buoyancy of the cloud. When different velocities to vapor and liquid phase are allowed, the liquid phase falls down faster due to gravity, leaving a cloud enriched in vapor phase of the components, and leading to a lighter mixture. The presence of humidity enhances the slip effect, because the liquefied and solidified water covers a much larger area in the domain than the liquid hydrogen, and therefore the main contribution to the buoyancy of the cloud comes from the humidity.

The predicted hydrogen concentration on the xz plane along the release is in very good agreement with the experiment for case 4, as shown in the group of diagrams in Fig. 3. The oscillations of hydrogen concentration for case 3 and 4 are captured quite well, although an approximation of the wind direction was taken. The highest deviations from the average wind direction are capable to describe the physical phenomenon, so, at the time there is no need in modeling every fluctuation. However, the arrival time of the peaks is underestimated. More data about the exact location of the wind direction measurement and measurements in more locations would provide valuable information, especially for the initial wind field (at the start of the release), and consequently could improve the arrival time of the peaks and the prediction.

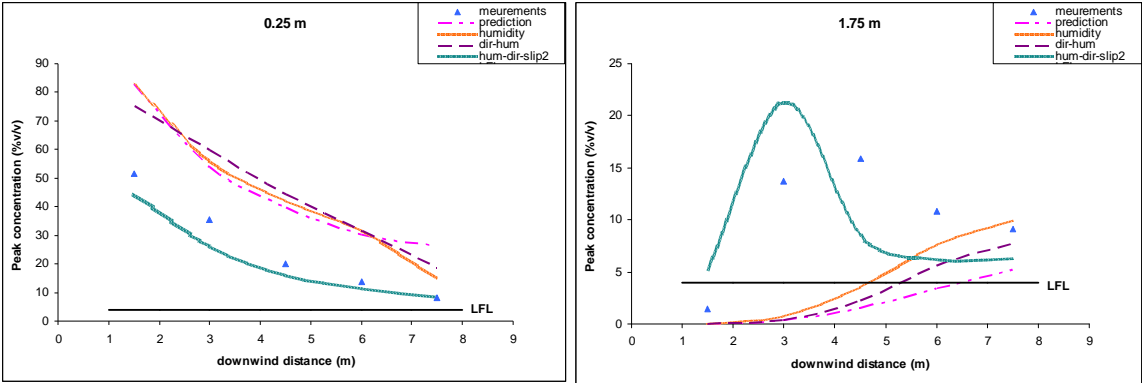


Figure 2. The predicted and measured peak concentration for test 5 at distances downwind the release, at  $y=0$ , and at heights above ground, a) 0.25 m, and b) 1.75 m.

In cases 1 and 2 where the wind direction was assumed in line with the release the respective time histories are approximately a straight line. This behavior confirms that the fluctuations of wind direction in these experiments influence to a great extent the gas dispersion, and they should not be neglected.

Furthermore, in Fig. 3 it is shown that hydrogen concentration has a peak at about 6 seconds after the start of the release for case 1 and 2. This peak is due to the heat transfer from the ground. At initial stage of the release the cloud absorbs large amount of heat, because of the high temperature difference between it and the ground. Then the rate of heat transfer is decreased as the ground becomes colder, leading to a larger cryogenic pool. The vaporization rate is smaller, and therefore the concentration levels become lower. This ground heat transfer effect is significant in test 5. In test 6 the effect is smaller, because of the position and the direction of the spill point, which at 100mm height with vertical direction. So, the cloud is delayed to come in contact with the ground, and when it reaches the ground is already heated by the environment. In test 7, there is no such peak, because the spill point is even higher and the cloud touches the ground far away when it is warmer.

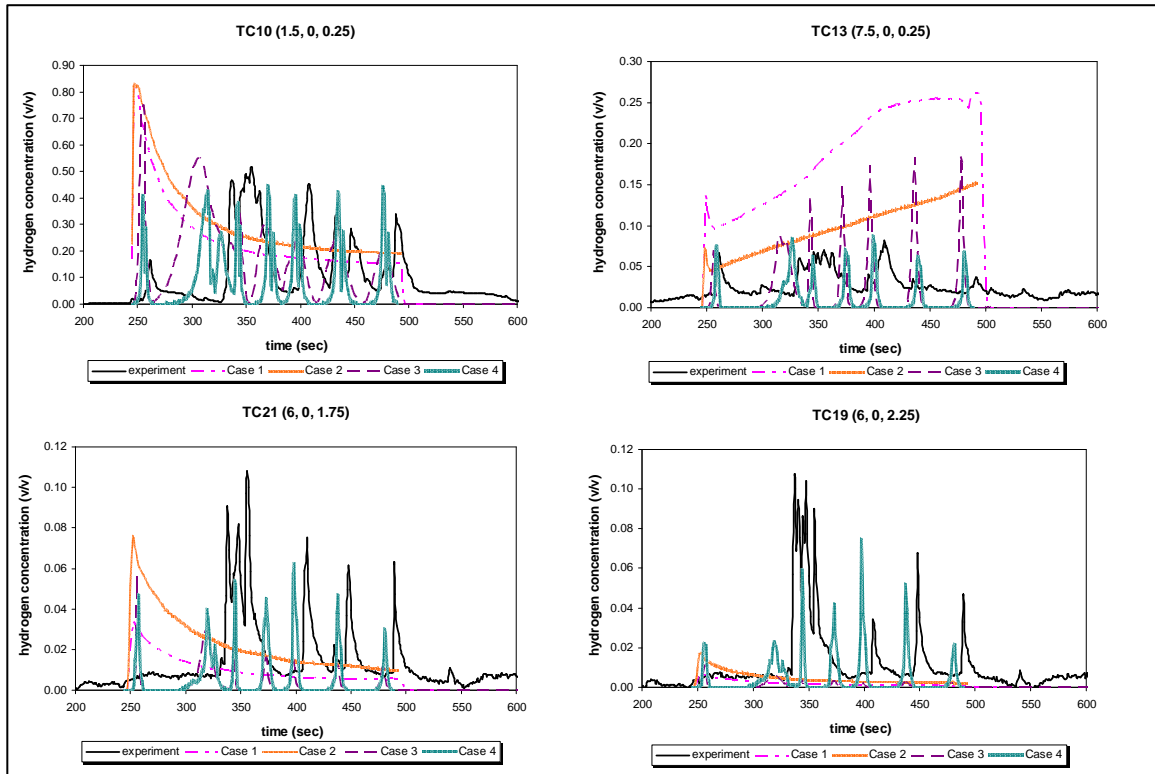


Figure 3. Time histories of predicted hydrogen concentration for test 5 for all simulation cases compared with the experiment at several downwind distances and heights. The exact location of the sensors ( $x, y, z$  coordinates, in respect with the release point located at  $x=0$ , and  $y=0$ , and the ground level at  $z=0$ ) is shown in the parenthesis.

Finally, the complex surrounding terrain with hills and vegetation generates high turbulence levels that affect the mixing process and consequently the gas dispersion. In the simulation this generated turbulence is not taken into account and could be a reason of the not so well predicted concentration in some sensors.

#### 4.2 Test 6

Fig. 4 indicates the importance of slip effect along with the humidity and wind direction effect on the numerical results. The predicted maximum hydrogen concentration in distances downwind the release is compared with the measured one. In case 1 the results give overprediction of concentration and the trend is not similar to the experiment for sensors at lower heights. In the experiment concentration is constantly reduced downwind the release, while in prediction concentration is increased with increasing distance from the release point until 4.5 m, where it starts to decrease. On the contrary, case 4 underestimates the maximum concentration, but it fits the trend pretty well. Despite the underprediction the model still gives concentration levels above lower flammability limit (LFL=4%) for the sensors near the release. At the higher sensor, case 4 still gives a good prediction, though it overpredicts the concentration levels near the release point.



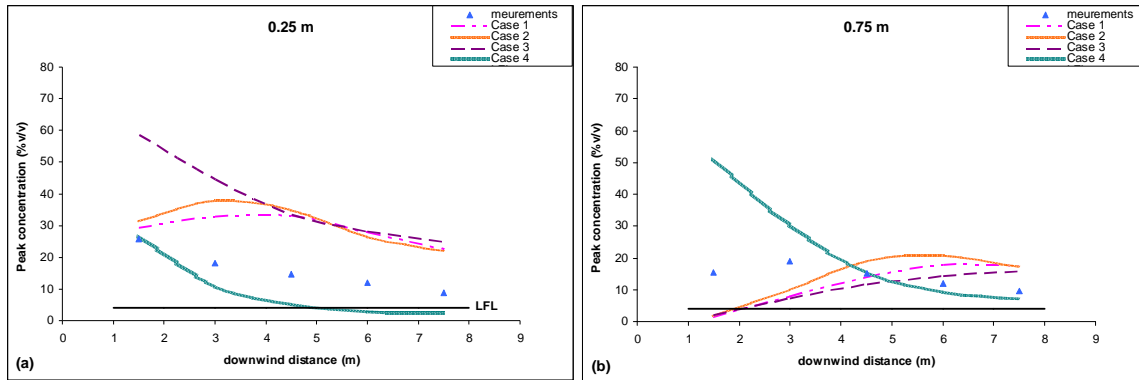


Figure 4. The predicted and measured peak concentration for test 6 at distances downwind the release, at  $y=0$ , and at heights above ground, a) 0.25 m, and b) 0.75 m.

As mentioned in the previous section, the effect of air condensation/solidification on the buoyancy of the cloud along with the humidity solidification effect should be examined in the future though it is expected to be small.

### 4.3 Test 7

Similar remarks with test 5 and 6 can be made for test 7 too. The predicted maximum hydrogen concentration for each case in distances downwind the release compared to the measured ones are displayed in Fig.5. In all three cases the model overestimates the hydrogen concentration for most of the lower sensor by approximately a factor of 2. For the higher sensor the prediction is in very good agreement for all cases, but still gives overestimated concentration near the release point. This behavior implies that the predicted cloud is less buoyant than the experimental cloud. The slip effect would make the cloud more buoyant, as it is concluded in the previous tests.

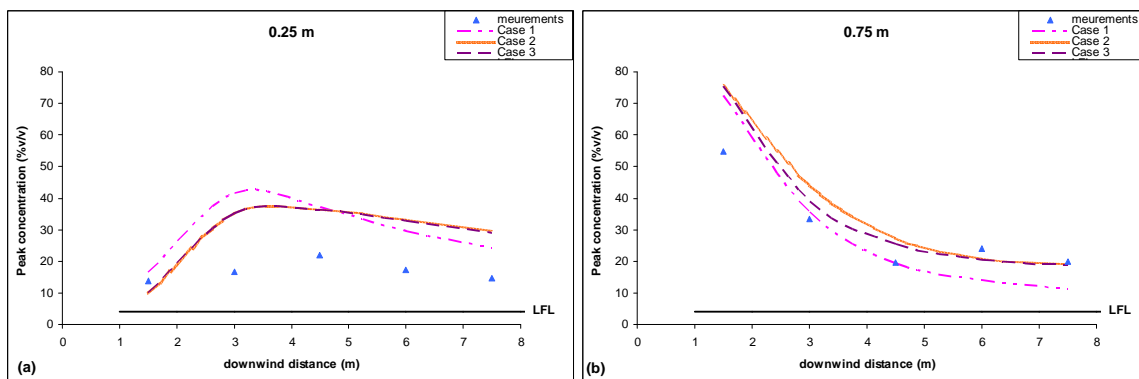


Figure 5. The predicted and measured peak concentration for test 7 at distances downwind the release, at  $y=0$ , and at heights above ground, a) 0.25 m, and b) 0.75 m.

## 5.0 CONCLUSIONS AND FUTURE WORK

Three tests were simulated with the CFD code ADREA-HF related to liquefied hydrogen (LH<sub>2</sub>) dispersion. The experiments were performed by the Health and Safety Laboratory in 2010. The spill point, direction and duration are different in each test, while the spill rate is 60lt/min for all three tests. Sensors measured the temperature at several distances downwind the release and several heights above the ground. The hydrogen concentration was deduced by the measured temperature assuming adiabatic mixing.

The parameters that influence the simulation of LH2 dispersion, and that were examined in this study are the following: the air moisture, the wind direction, and the consideration of the slip velocity between the vapor and non vapor phase (liquid and solid).

The presence of air moisture makes the cloud more buoyant, because of the heat liberation by the condensation and solidification of the water. The predicted concentration is in better agreement with the experiment in the case with humidity compared to the case without humidity.

The comparison between the predicted hydrogen concentration and the measured ones shows that wind direction affects the LH2 dispersion to a great extent. Assuming a constant wind direction equal to the average measured direction is not consistent with these experiments. It seems that the instantaneous wind shifts influence the cloud's direction, which fluctuates around the release line center. This behavior is due to the high oscillations in wind direction during large time intervals, giving the cloud enough time to correspond to them.

The slip effect has also a great impact on hydrogen dispersion, and cryogenic pool creation and spreading. When LH2 is spilled, a two phase release and multiphase flow are generated. At the release point the hydrogen is in both vapor and liquid phase due to flash vaporization. The liquid phase is dispersed in the domain in the form of droplets, and of cryogenic pool when it touches the ground. In the presence of air moisture the water is converted to liquid and even solid because of the very low prevailed temperature. The gravity forces the vapor phase and non vapor phase of both hydrogen and water to obtain different velocities, and their difference is called slip velocity. When slip velocity is taken under consideration in the simulation the non vapor phase falls fast to the ground, resulting to a lighter, more buoyant cloud. The prediction with the slip effect is in very good agreement with the experiment, and has been improved compared with the case with homogeneous equilibrium model assumption. In most of the sensors presented here the relative error of the maximum predicted concentration with slip effect has been decreased about 1%- 125% from the respective one without slip consideration for both test 5 and 6.

For the best simulation case (air moisture, fluctuating wind direction, and slip velocity) of test 5 and 6 the prediction is consistent with the measurements. However, in test 5 the model underpredicts the hydrogen concentration for most of sensors. In test 6 the model underpredicts the hydrogen concentration at low sensors, and overpredicts it at higher sensors.

Finally, in test 7 the model overpredicts the hydrogen concentration at lower sensors for all three cases (homogeneous model without humidity and with wind direction in line with the release, homogeneous model with humidity and with wind direction in line with the release, homogeneous model with humidity and transient wind direction) and underpredicts it at higher sensors. This behavior indicates that the predicted cloud is less buoyant than the experimental one. A consideration of slip effect could make the cloud more buoyant and the prediction would be closer to the experiment.

The effect of condensation/solidification of the air components (N<sub>2</sub> and O<sub>2</sub>) on the buoyancy of the cloud should be examined for test 5 and 6 combined with the respective humidity effect. For test 7, the effect of air condensation is small, as concluded in [17], and therefore, it is not necessary to be taken into account.

In the future, the wind direction can be modeled more accurately. In the present work, the vertical profile of v-component is uniform. The effect of a non uniform profile should be tested. As far as the slip effect concerned, other slip models can be studied, in order to improve the prediction. In addition, u- and v-slip components should be incorporated to the model, and their influence should be examined. Finally, the heat flux from the ground to the cryogenic pool according to the hydrogen boiling curve will be implemented to the ADREA-HF code, and will be tested for its effect on vapor dispersion.

## ACKNOWLEDGEMENT

Authors acknowledge the support of this work by the H2FC project (Grant agreement No 284522 'Integrating European Infrastructure to support science and development of Hydrogen- and Fuel Cell Technologies towards European Strategy for Sustainable, Competitive and Secure Energy').

## REFERENCES

1. Hooker, P., Willoughby, D.B. and Royle, M., Example, Experimental Releases of Liquid Hydrogen, 4<sup>th</sup> International Conference on Hydrogen Safety, San Francisco, Paper 160, 2011.
2. Venetsanos, A.G., Papanikolaou, E. and Bartzis, J.G., The ADREA-HF CFD Code for Consequence Assessment of Hydrogen Applications, *Hydrogen Energy Journal*, **35**, 2010, pp. 3908-3918.
3. Bartzis, J.G., ADREA-HF: A Three Dimensional Finite Volume Code for Vapour Cloud Dispersion in Complex Terrain, Report EUR 13580 (1991).
4. Würtz, J., Bartzis, J.G., Venetsanos, A.G., Andronopoulos, S., Statharas, J. and Nijsing, R., A Dense Vapour Dispersion Code Package for Applications in the Chemical and Process Industry, *Hazardous Material Journal*, **46**, No. 2-3, 1996, pp. 273-284.
5. Statharas, J.C., Venetsanos, A.G., Bartzis, J.G., Würtz, J. and Schmidtchen, U. Analysis of Data from Spilling Experiments Performed with Liquid Hydrogen, *Hazardous Material Journal*, **77**, No.1-3, 2000, pp. 57-75.
6. Venetsanos, A.G., Baraldi, D., Adams, P., Heggem, P.S. and Wilkening, H. CFD Modelling of Hydrogen Release, Dispersion and Combustion for Automotive Scenarios, *Loss Prevention in the Process Industries Journal*, **21**, 2008, pp. 162-184.
7. Baraldi, D., Venetsanos, A.G., Papanikolaou, E., Heitsch, M. and Dallas, V., Numerical Analysis of Release, Dispersion and Combustion of Liquid Hydrogen in a Mock-up Hydrogen Refuelling Station, *Journal Loss Prevention in the Process Industries*, **22**, 2009, pp. 303-315.
8. Venetsanos, A.G., and Bartzis, J.G., CFD Modeling of Large-Scale LH2 Spills in Open Environment, *Hydrogen Energy Journal*, **32**, 2007, pp. 2171-2177.
9. Giannissi, S.G., Venetsanos, A.G., Markatos, N. and Bartzis, J.G, Numerical Simulation of LNG Dispersion under Two-Phase Release Conditions, *Journal of Loss Prevention in the Process Industries*, **26**, No. 1, 2013, pp. 245-254.
10. Statharas, J.C., Bartzis, J.G., Venetsanos, A. and Wurtz, J., Prediction of Ammonia Releases using ADREA-HF Code, *Process Safety Progress Journal*, **12**, No. 2, 1993, pp. 118-122.
11. Andronopoulos, S., Bartzis, J.G., Würtz, J. and Asimakopoulos, D., Modelling the Effects of Obstacles on the Dispersion of Denser-than-Air Gases, *Hazardous Material Journal*, **37**, No. 2, 1994, pp. 327-352.
12. Andronopoulos, S., Stratharas, J.C., Deligiannis, P. and Bartzis, J.G., Evaluation of the Predictions of the ADREA-HF Code for Dense Gas Dispersion with Real Scale Ammonia Release Experiments, 4<sup>th</sup> International Conference on Air Pollution, Toulouse, Code 45563, 1996, pp. 81-86.
13. Markatos, N.C., Malin, M.R. and Cox, G., Mathematical Modelling of Buoyancy-Induced Smoke Flow in Enclosures, *Heat Mass Transfer Journal*, **25**, 1982, pp. 63-75.
14. Venetsanos, A.G., Papanikolaou, E. and Bartzis, J.G., The ADREA-HF CFD code for Consequence Assessment of Hydrogen Applications, *Hydrogen Energy Journal*, **35**, 2010, pp. 3908-3918.
15. Giannissi, S.G., Venetsanos, A.G., Bartzis, J.G, Markatos, N., Willoughby, D.B. and Royle, M., CFD Modeling of LH2 Dispersion using the ADREA-HF code, 4<sup>th</sup> International Conference on Hydrogen Safety, San Francisco, Paper 196, 2011.
16. Ogura Y. and Takahashi T., Numerical Simulation of the Life Cycle of a Thunderstorm Cell, *Monthly Weather Review Journal*, **99**, 1971, pp. 895-911.

17. Ichard, M., Hansen, O.R. , Middha, P. and Willoughby, D., CFD Computations of Liquid Hydrogen Releases, *Journal of Hydrogen Energy*, **37**, 2012, pp. 17380-17389.